Journal of Ceramic Processing Research. Vol. 23, No. 3, pp. 278~286 (2022)
(Received 18 October 2021, Received in revised form 25 January 2022, Accepted 27 January 2022)
https://doi.org/10.36410/jcpr.2022.23.3.278

J O U R N A L O F
Ceramic Processing Research

Optimization of CO_2 laser welding process parameters on cupronickel alloys using multi-objective techniques

S. Karthick[a]*, V. Paramasivam[b], V Mohanavel[c,d] and K. Arul[e]
[a]*Department of Mechanical Engineering, J.J. College of Engineering and Technology, Tiruchirappalli - 620009, Tamil Nadu, India*
[b]*Department of Mechanical Engineering, PSNA College of Engineering and Technology, Dindigul- 624622, Tamil Nadu, India*
[c]*Centre for Materials Engineering and RegenerativeMedicine, Bharath Institute of Higher Education and Research, Chennai - 600 073, Tamil Nadu, India*
[d]*Department of Mechanical Engineering, Chandigarh University,Mohali-140413, Punjab, India*
[e]*Department of Mechanical Engineering, Agni College of Technology, Chennai - 600 130, Tamil Nadu, India*

Optimization of process parameters for welding cupronickel alloys using CO2 laser welding process was investigated in this study. Laser Beam Welding (LBW) process, is one of the beneficial techniques for airplane fastening. Turbine motor components were made up of superalloy because of its high specific, low heat input, high heat focus, high-power density, and low contortion. Using CO2 LBW process, welding can be done on a wide range of materials, especially alloys which are difficult to weld by conventional welding process. This investigation focuses on optimizing the LBW process parameters of cupronickel alloys utilizing multi criteria decision making (MCDM) methodology and TOPSIS analysis. The input parameters like laser power, welding speed, welding angle and welding current are preferred as the fundamental part to enhance the welding. Welding process is carried out on 16 specimens in order to improve and support mechanical and metallurgical qualities of the welded parts. Welding is made with four input variables in two levels of values. TOPSIS has been employed as a statistical design tool to identify the most significant parameters on the overall Multiobjective function. Among the experiments, the best mechanical properties were observed in welding made with the parameters like Welding current (900 W), Welding angle (90°), Welding speed (1.4mm/min) and Laser power (30 W). This investigation strives to reveal the better process parameters, mechanical properties and energy consumption of CO_2 LBW welded elements of cupronickel alloy.

Keywords: Energy consumption, Laser beam welding, CO_2 laser, TOPSIS, Mechanical properties.

Introduction

The advantages of laser beam welding include low and precise heat input, a restricted heat affected zone, and little distortion. High-speed welding can also be used to automate the process. When compared to other welding techniques, laser welding offers various potential benefits, including deeper penetration, faster welding speed, high precision, dependability, efficiency, and productivity. Due to their mechanical qualities, dissimilar metals such as Austenitic stainless steel and low carbon steel are commonly used in power generating applications [1-4]. The use of different metal combinations allows for a more versatile product design by maximizing the use of each material. Intricate structures and complex joints of thin to thick materials can also be used with laser beam welding. High power welding processes has become popular in industrial manufacturing in recent years due to their numerous advantages, including minor shape distortions, reduced heat affected zone (HAZ) size, faster welding speed associated with high penetrations, and a high 'depth to width ratio' for the fusion zone (FZ). These include the absence of filler materials, elimination of edge preparation, ability to weld near heat-sensitive elements (e.g. electronic circuits), and presence of a minimum amount of porosity and contaminants [5-8]. Cupronickel alloys are one of the finest materials which are having wide range of applications in recent industrial and manufacturing sectors majorly in marine applications. The practical applications of the considered alloys, encourages the researchers and academicians to investigate their characteristics under various conditions [9-12]. Welding of cupronickel alloys gained more attention among research practitioners. However, unexpected failures become more common in welding operations which might be due the impact of various factors like the type of welding, welding environment and its process parameters. Welding of cupronickel alloys with gas tungsten arc welding and gas metal arc welding

*Corresponding author:
Tel : +919788220668
E-mail: skarthick1480@gmail.com

increases the porosity which results in material losses. Also, very few literatures were reported on cupronickel alloy with CO_2 laser beam welding [13-16]. Hence, this study sought to explore the effectiveness of cupronickel alloy welding using CO_2 laser beam welding by varying the process parameters. Process parameters of welding are essential and directly proportional to the strength of welded joint. Optimization of process parameters can improve the quality, life and reliability of weld. The parameter optimization in CO_2 laser beam welding is not a new concept [17-20]. Four process parameters were optimized in CO_2 laser beam welding in the application of AM60 magnesium-based alloy. Each process parameters (laser power, welding speed, focal point position and gas flow rate) has two levels of examination. These parameters were optimized based on the heat affected zone, hardness values and its metallurgical observations [21-23]. Fusion reactor material (SS 316L) welding characterization done by CO_2 laser beam welding by varying process parameters including laser power, speed and further examined with the assistance of radiography, non-destructive test and ultrasonic test. In addition, the weld samples mechanical properties like tensile, bend and fracture strength were are explored. Heat fusion zone, micro structural properties, mechanical strength like tensile, flexural, impacts and hardness were explored in weld joint of nickel-based alloy 825 using CO_2 laser beam welding. Praising with development of CO_2 laser, some studies consider the impact of CO_2 laser beam welding combined with other welding systems as a hybrid welding, for an instance; Process parameters of hybrid welding system which includes CO_2 laser and metal active gas (MAG) on E36 steel material [24-26]. In this study, they have explored the different positions of droplet transfers which include flat, vertical and horizontal positions to optimize considered welding process parameters. A model to deal with the weld pool dynamics through hybrid laser welding system (CO_2 laser, tungsten inert gas (TIG) +CO_2 laser). They proposed a numerical method, further validated with experiments and simulation with S-235JR. The above literatures reveal that CO_2 laser has great potential in welding research, in addition, it proves that, still there is enough room to explore on CO_2 laser beam welding with different materials [27, 28]. With this concern, this study considers cupronickel alloys, which has wide range of applications as mentioned earlier. Only very few studies explored the welding properties of cupronickel alloys, for an instance, Argon arc welding behavior of aluminium bronzes and copper nickel alloys joints. This study sought to improve the weld quality through crack free joints by adding copper nickel welding wire with optimized percentage of inclusion. In addition, they have studied the mechanical properties of the weld specimen with different weld wire percentages. The melt run trials' experimental results were acquired by adjusting the laser power and welding speed. These findings were used to represent the laser source properties in a correct numerical model and to compute the thermal field in the material at every instant. This type of analysis is extremely tough to carry out due to the phenomenon's complexity. Parameters of CO_2 laser beam welding of copper nickel alloys with the assistance of both experimental and numerical model. The considered parameters include laser power and welding speed, further the microstructural properties were tested along with mechanical properties. Finite element analysis is used as numerical method to identify the obtained results as reliable. Welding parameters of CO_2 laser beam welding on 70/30 cupronickel alloys. This study varies the welding speeds ranges from 1.0 m/min to 2.5 m/min with 0.5 increments, Mechanical properties of the welded joints were explored based on the above different welding speeds [29]. Finally, based on the results of tensile, hardness and elongation, it has been concluded that 1.5 m/min welding speed features best characteristics. Though few studies do consider the welding process parameters, since they are limited with the consideration of multi parameters and in addition, most of the studies are limited with old methodologies. Hence, in this study, CO_2 laser beam welding process parameters in the application of renowned material cupronickel alloy with novel integration of multi criteria decision making (MCDM) methodology, TOPSIS.

Materials and Methods

Base material

Cupronickel 90/10 (CuNi10Fe1Mn) were used in this investigation. The chemical composition of considered material is shown in Table 1. Rectangular sample plates with the dimensions of $100 \times 100 \times 1.9$ mm^3 were prepared and properly aligned in the fixtures of CO_2 laser welding machine.

Experimental analysis

Table 2 shows the process parameters and range of levels considered for the study. Based on these parameters, butt joints were made with CO_2 laser beam welding on similar cupronickel alloy. Fig. 1 and 2

Table 1. Chemical composition of 90/10 Cupronickel alloy

Chemicals	Ni	Fe	Mn	Cu
Composition	10.12	1.58	0.78	Rem.

Table 2. Considered process parameters of CO_2 laser beam welding on cupronickel alloys

Process parameters	Unit	Level I	Level II
Welding current (I)	A	900	500
welding Angle (D)	◦	45	90
Welding Speed (S)	mm/min	1	1.4
Laser power (P)	W	20	30

Table 3. Different combinations of process parameters considered for the study

Alternatives	I	D	S	P
W1	500	45	1	20
W2	500	90	1	20
W3	500	90	1.4	20
W4	500	90	1.4	30
W5	900	90	1.4	30
W6	500	45	1.4	30
W7	900	90	1	30
W8	500	45	1.4	20
W9	500	90	1	30
W10	900	90	1.4	20
W11	900	45	1.4	30
W12	500	45	1	30
W13	900	90	1	20
W14	900	45	1.4	20
W15	900	45	1	30
W16	900	45	1	20

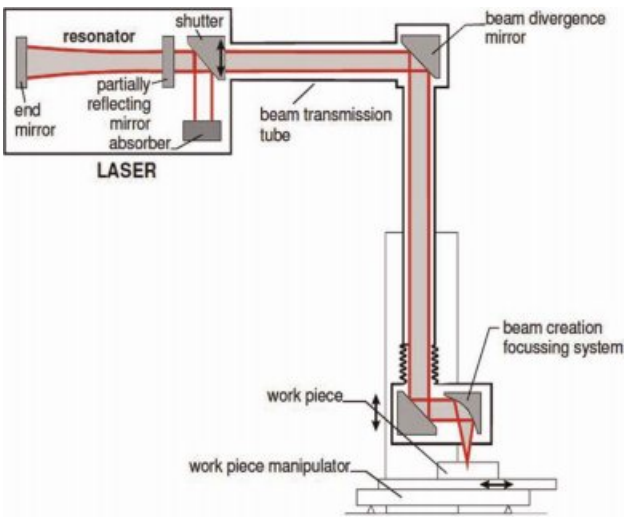

Fig. 1. Laser welding machine - A schematic representation.

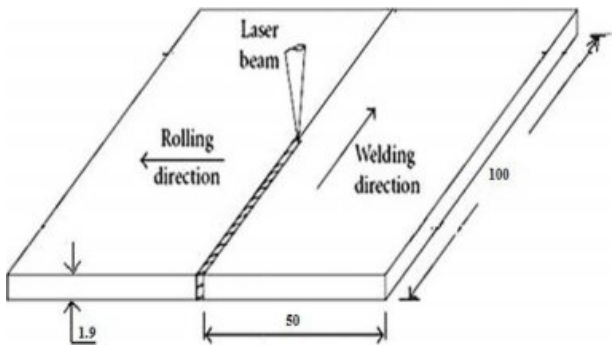

Fig. 2. Butt weld specimen dimensions.

shows the schematic representation of CO_2 laser beam welding process and dimension of the specimen used. Helium is used as shielding gas (40 L/min) to protect molten bath during welding.

Three different types of experiments were carried out and for each investigation, required standard and procedures were practiced as discussed below.

Tensile test

The weld specimens were subjected to tensile load in order to identify its yield strength, tensile strength and % of elongation. The experiment was conducted on ultimate tensile machine with the capacity of 100 kN based on ASME. The results are recorded and processed in numerical model as one of the evaluation criteria for process parameters.

Hardness

Vickers hardness was examined on three zones namely base metal zone, HAZ and weld zone. Different trails have been made and average value was considered. The experimental outputs are included in the numerical part for further analysis.

Impact test

This test helps to compare the impact properties of weld material with the base metal. The weld specimen was reduced to the dimension suitable for Charpy V-notch test. All the above experimental results are processed through TOPSIS.

Numerical analysis

Many studies focus mainly the experimental programs to prove the reliability of the results whereas some studies compared the experimental and numerical methods. Most of the studies employed Taguchi method or other design of experiment techniques to analyze the process parameter optimization problem. But in virtual applications considering two or three process parameters couldn't provide clear picture. Hence researchers are in the quest to deal with these multi criteria problems existing in the welding process. Minding this gap, a novel approach (MCDM) was introduced in this study in addition with experimental investigations. Among MCDM tools, there are different strategies exist to evaluate the alternatives, (here different combination of welding parameters is considered as alternatives) and TOPSIS is one of the tools which highly suitable for dealing with multi criteria problems especially under the pressure of various factors. TOPSIS was pioneered by Hwang and Yoon (1981). After this introduction, many researchers adapted TOPSIS in their study. With these considerations, this study employed TOPSIS as a numerical method in combination with experimental investigations to improve reliability and in addition with dealing huge number of process parameters.

Steps involved in TOPSIS methodology is discussed below.

Step 1: Set up initial comparison matrix

In this step, an initial matrix will be formed, in which

the alternatives are filled with the weights/values of the concern criteria.

Step 2: Normalized matrix

Next step is to normalize the initial matrix derived from previous steps. Eq. (1) is used to derive normalized matrix, in which all values are between 0 to 1.

$$r_{ij} = \frac{x_{ij}}{\sqrt{\sum_{i=1}^{m} x_{ij}^2}} \tag{1}$$

Step 3: Weighted normalized matrix

To obtain weighted matrix, assigned weights of each criteria will be manipulated with each and every element in normalized matrix, shown as eq. (2).

$$V = \begin{bmatrix} v_{11} & v_{12} & \cdots & v_{1j} & \cdots & v_{1n} \\ \vdots & \vdots & & \vdots & & \vdots \\ v_{i1} & v_{i2} & & v_{ij} & & v_{in} \\ \vdots & \vdots & & \vdots & & \vdots \\ v_{m1} & v_{m2} & \cdots & v_{mj} & \cdots & v_{mn} \end{bmatrix} = \begin{bmatrix} w_1 r_{11} & w_2 r_{12} & \cdots & w_j r_{1j} & \cdots & w_n r_{1n} \\ \vdots & \vdots & & \vdots & & \vdots \\ w_1 r_{i1} & w_2 r_{i2} & & w_j r_{ij} & & w_n r_{in} \\ \vdots & \vdots & & \vdots & & \vdots \\ w_1 r_{m1} & w_2 r_{m2} & \cdots & w_j r_{mj} & \cdots & w_n r_{mn} \end{bmatrix} \tag{2}$$

Step 4: Distance between positive and negative solutions

In this step, it is necessary to find out the ideal and negative solution and their distances. D^+/S_i^+ and D^-/S_i^- are the distance between positive and negative solutions respectively, which is shown in eq. (3) and (4).

$$S_i^+ = \sqrt{\sum_{j=1}^{n} (v_{ij} - v_j^+)^2}\; i = 1,2,3 \ldots m \tag{3}$$

$$S_i^- = \sqrt{\sum_{j=1}^{n} (v_{ij} - v_j^-)^2}\; i = 1,2,3 \ldots m \tag{4}$$

Step 5: Ranking of alternatives based on closeness coefficients.

From the ideal and worst distances, the closeness coefficient can be determined (shown in eqation (5)), based on these closeness coefficeint values, the alternatives will be ranked against one another.

$$\left.\begin{aligned} C_i^* &= \frac{S_i^-}{(S_i^+ + S_i^-)}, 0 < C_i^* < 1; i = 1,2 \ldots \ldots, m \\ C_i^* &= 1, if A_i = A^+ \\ C_i^* &= 0, if A_i = A^- \end{aligned}\right\} \tag{5}$$

Application of TOPSIS

The above steps of TOPSIS are detailed in this section with the problem application. Table 2 shows the process parameters of CO_2 laser beam welding on cupronickel alloys. The samples were made based on these combinations of process parameters. These samples are posed to experiments to identify their mechanical properties and these properties was given as input in TOPSIS which are shown in Table 4.

Next step is to normalize the matrix which should range between 0 to 1, Table 5 shows the intermediate and Table 6 shows the final normalized matrix.

The obtained normalized matrix is further converted

Table 4. Pairwise comparison among criteria over alternatives

Objective					Max	Max	Max	Min	Max
I	D	S	P	Alternatives	Hardness	Yield strength (MPa)	Tensile strength (MPa)	Elongation (%)	Charpy impact (J)
500	45	1	20	W1	200	320	410	11	85
500	90	1	20	W2	220	310	380	18	111
500	90	1.4	20	W3	180	288	402	21	68
500	90	1.4	30	W4	350	264	367	15	53
900	90	1.4	30	W5	315	310	424	9	58
500	45	1.4	30	W6	162	344	530	8	64
900	90	1	30	W7	154	266	521	13	102
500	45	1.4	20	W8	286	245	538	15	106
500	90	1	30	W9	154	232	343	20	92
900	90	1.4	20	W10	322	266	459	18	96
900	45	1.4	30	W11	232	290	416	11	83
500	45	1	30	W12	210	308	398	12	97
900	90	1	20	W13	342	311	534	15	76
900	45	1.4	20	W14	310	218	426	13	72
900	45	1	30	W15	324	254	315	19	91
900	45	1	20	W16	268	310	401	14	82
Assigned Weights					0.2	0.2	0.2	0.2	0.2
Solutions				ideal	350	344	538	8	111
				worst	154	218	315	21	53

Table 5. Normalized matrix (initial)

Alternatives	Hardness	Yield strength (MPa)	Tensile strength (MPa)	Elongation (%)	Charpy impact
W1	202	331	408	10	79
W2	224	319	375	3	108
W3	183	278	392	0	72
W4	356	258	371	6	63
W5	318	320	418	12	61
W6	168	339	528	13	71
W7	158	259	519	8	106
W8	290	252	529	6	112
W9	161	241	336	1	102
W10	319	271	442	3	89
W11	229	298	406	10	91
W12	218	316	386	9	89
W13	346	309	528	6	81
W14	318	223	419	8	86
W15	328	249	325	2	89
W16	267	308	399	7	93
$\sum x_{ij}^2$	1089469	1304762	3016802	902	116022
$(\sum x_{ij}^2)^{1/2}$	1043.776317	1142.261791	1736.894355	30.03331484	340.6200229

Table 6. Normalized matrix (final)

Alternatives	Hardness	Yield strength (MPa)	Tensile strength (MPa)	Elongation (%)	Charpy impact
W1	0.191611826	0.280144521	0.236048621	0.332963579	0.249552316
W2	0.210774109	0.271361422	0.218771526	0.099889074	0.325862351
W3	0.172451124	0.252142316	0.231432561	0	0.199635945
W4	0.335320887	0.231120398	0.211296674	0.199778147	0.155598604
W5	0.301788798	0.271391377	0.244113868	0.399556295	0.170277717
W6	0.155205667	0.301156882	0.305142336	0.432852653	0.187892654
W7	0.14754119	0.23287131	0.299960673	0.266370863	0.299453917
W8	0.274005067	0.214486733	0.309748258	0.199778147	0.311197208
W9	0.14754119	0.203105804	0.197478908	0.033296358	0.27009569
W10	0.308495216	0.23287131	0.264264777	0.099889074	0.281838981
W11	0.222269845	0.253882256	0.239507946	0.332963579	0.243673285
W12	0.201192532	0.269640464	0.229144622	0.299667221	0.284774803
W13	0.327656409	0.272266833	0.307445297	0.199778147	0.223122526
W14	0.2969985	0.19084942	0.245265349	0.266370863	0.211379235
W15	0.310411335	0.222365838	0.181358181	0.066592716	0.267159867
W16	0.256759993	0.271391377	0.230871843	0.233074505	0.240737463

Table 7. Weighted normalized matrix

Alternatives	Hardness	Yield strength (MPa)	Tensile strength (MPa)	Elongation (%)	Charpy impact
W1	0.038322387	0.056029187	0.047210701	0.066592716	0.049908986
W2	0.042154626	0.054278275	0.043756259	0.019977815	0.065175264
W3	0.034490148	0.050426269	0.046289517	0	0.039927189
W4	0.067064177	0.04622408	0.042259335	0.039955629	0.031119721
W5	0.06035776	0.054278275	0.048822774	0.079911259	0.034055543
W6	0.031041133	0.060231376	0.061028467	0.086570531	0.037578531
W7	0.029508238	0.046574262	0.059992135	0.053274173	0.059890783
W8	0.054801013	0.042897347	0.061949652	0.039955629	0.062239442
W9	0.029508238	0.040621161	0.039495782	0.006659272	0.054019138
W10	0.061699043	0.046574262	0.052852955	0.019977815	0.056367796
W11	0.044453969	0.050776451	0.047901589	0.066592716	0.048734657
W12	0.040238506	0.053928093	0.045828924	0.059933444	0.056954961
W13	0.065531282	0.054453367	0.061489059	0.039955629	0.044624505
W14	0.0593997	0.038169884	0.04905307	0.053274173	0.042275847
W15	0.062082267	0.044473168	0.036271636	0.013318543	0.053431973
W16	0.051351999	0.054278275	0.046174369	0.046614901	0.048147493
Ideal	0.067064177	0.060231376	0.061949652	0.086570531	0.065175264
Worst	0.029508238	0.038169884	0.036271636	0	0.031119721

Table 8. From ideal solution

Alternatives	Hardness	Yield strength (MPa)	Tensile strength (MPa)	Elongation (%)	Charpy impact
W1	0.02874179	0.004202189	0.013020675	0.019977815	0.015266278
W2	0.024909551	0.005953101	0.016475117	0.066592716	-2.46152E-10
W3	0.032574029	0.009805107	0.013941859	0.086570531	0.025248075
W4	-3.12383E-10	0.014007296	0.017972041	0.046614902	0.034055543
W5	0.006706417	0.005953101	0.011408602	0.006659272	0.031119721
W6	0.036023044	-4.85167E-10	-0.000797091	4.32437E-10	0.027596733
W7	0.037555939	0.013657114	0.000239241	0.033296358	0.005284481
W8	0.012263164	0.017334029	-0.001718276	0.046614902	0.002935822
W9	0.037555939	0.019610215	0.020735594	0.079911259	0.011156126
W10	0.005365134	0.013657114	0.007378421	0.066592716	0.008807468
W11	0.022610208	0.009454925	0.012329787	0.019977815	0.016440607
W12	0.026825671	0.006303283	0.014402452	0.026637087	0.008220303
W13	0.001532895	0.005778009	-0.001257683	0.046614902	0.020550759
W14	0.007664477	0.022061492	0.011178306	0.033296358	0.022899417
W15	0.00498191	0.015758208	0.02395974	0.073251988	0.011743291
W16	0.015712178	0.005953101	0.014057007	0.03995563	0.017027771

Table 9. From worst solution

Alternatives	Hardness	Yield strength (MPa)	Tensile strength (MPa)	Elongation (%)	Charpy impact
W1	0.008814149	0.017859303	0.010939065	0.066592716	0.018789265
W2	0.012646388	0.016108391	0.007484623	0.019977815	0.034055543
W3	0.00498191	0.012256385	0.010017881	0	0.008807468
W4	0.037555939	0.008054196	0.005987699	0.039955629	-2.33819E-10
W5	0.030849522	0.016108391	0.012551138	0.079911259	0.002935822
W6	0.001532895	0.022061492	0.024756831	0.086570531	0.00645881
W7	1.74485E-11	0.008404378	0.023720499	0.053274173	0.028771062
W8	0.025292775	0.004727463	0.025678016	0.039955629	0.031119721
W9	1.74485E-11	0.002451277	0.003224146	0.006659272	0.022899417
W10	0.032190805	0.008404378	0.016581319	0.019977815	0.025248075
W11	0.014945731	0.012606567	0.011629953	0.066592716	0.017614936
W12	0.010730268	0.015758209	0.009557288	0.059933444	0.02583524
W13	0.036023044	0.016283483	0.025217423	0.039955629	0.013504784
W14	0.029891462	-6.46327E-11	0.012781434	0.053274173	0.011156126
W15	0.032574029	0.006303284	1.09094E-10	0.013318543	0.022312252
W16	0.021843761	0.016108391	0.009902733	0.046614901	0.017027772

into weighted normalized matrix by multiplying the weights of corresponding criteria. Here from the advice of experienced welding technician, all the criteria weights are considered as equal and their summation should be equal to 1. The weighted normalized matrix is shown in Table 7.

Table 8 and 9 evidences the matrix form with the use of the best and worst weighted normalized matrix solutions.

From the above tables, we have to found out the distance between negative and positive solutions of the problem. The positive and negative distances are shown in Table 10 along with closeness coefficient Cc_i.

Results and Discussion

From the numerical analysis based on the mechanical properties of different sample of CO_2 laser beam welding on cupronickel alloys, the following rankings has been made (see Table 11) with the assistance of TOPSIS.

Table 11 reveals that welding specimen "**W5**" (Welding current 900 A, Welding angle 90º, Welding speed 1.4 mm/min and Laser power 30 w) gained more weight and on the other hand, "**W9**" (Welding current 500 A, Welding angle 90º, Welding speed 1 mm/min and Laser power 30 w) gained less weight. It shows that the optimum selection of process parameters can improve the results up to 50 percent than the least optimal solution. Also, from the results it can be seen that welding current plays a vital role in mechanical characteristics of weld specimen. Because in both best and worst cases of process parameters, the only difference is welding current. In addition, other weld specimen results show

Table 10. Distance between positive and negative solutions

Alternatives	D^+	D^-	Cc_i
W1	0.040564	0.072828	0.642266401
W2	0.073225	0.045103	0.381170848
W3	0.097383	0.018787	0.161722649
W4	0.062064	0.055746	0.47318632
W5	0.034976	0.088109	0.715834995
W6	0.045386	0.092942	0.671895496
W7	0.052284	0.065568	0.556361044
W8	0.051336	0.06234	0.548402732
W9	0.093463	0.02419	0.205602243
W10	0.069151	0.049177	0.41559906
W11	0.03771	0.072543	0.657967056
W12	0.04176	0.068661	0.621810478
W13	0.051309	0.063068	0.551404868
W14	0.047994	0.063399	0.569147133
W15	0.079693	0.042143	0.345898652
W16	0.048645	0.057425	0.541387597

Table 11. Rankings of alternatives

I	D	S	P	Alternatives (Welding samples)	Cci	Rank
500	45	1	20	W1	0.642266401	4
500	90	1	20	W2	0.381170848	13
500	90	1.4	20	W3	0.161722649	16
500	90	1.4	30	W4	0.47318632	11
900	**90**	**1.4**	**30**	**W5**	**0.715834995**	**1**
500	45	1.4	30	W6	0.671895496	2
900	90	1	30	W7	0.556361044	7
500	45	1.4	20	W8	0.548402732	9
500	90	1	30	W9	0.205602243	15
900	90	1.4	20	W10	0.41559906	12
900	45	1.4	30	W11	0.657967056	3
500	45	1	30	W12	0.621810478	5
900	90	1	20	W13	0.551404868	8
900	45	1.4	20	W14	0.569147133	6
900	45	1	30	W15	0.345898652	14
900	45	1	20	W16	0.541387597	10

the difference in the result which mainly affect with the laser power. Hence, sensitivity analysis on laser power can improve more option in finding appropriate solution.

Thermal Distribution using Ansys Simulations

Studies of the thermal distribution during welding process are analyzed by ANSYS 18.1 version. For this study the foremost important factors such as the thermal conductivity, density and specific heat are considered for the weld materials. Weld material meshing plays a very important role for the better result. Fig. 3 show the concept of meshing of weld materials.

For the welding speed of 3 mm/sec the ANSYS simulation was analyzed at constant heat input 1,600

Fig. 3. Meshing on the Single Plate.

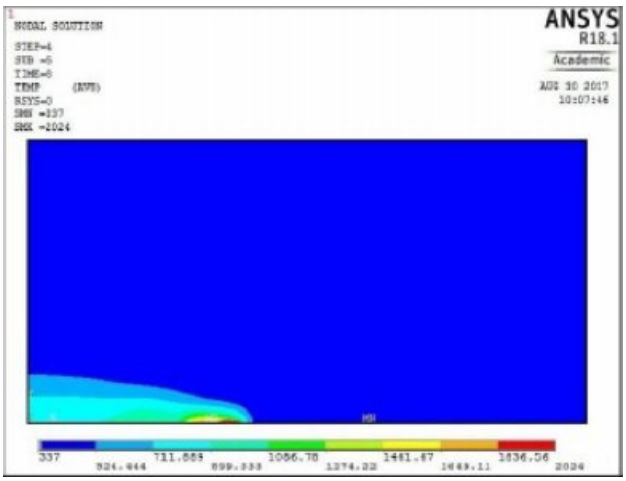

Fig. 4. Temperature profile of AISI304 and SA213T22 TIG Welding.

J/mm. Let us consider the weld efficiency is around 86% and the temperature profile was analysed as represented in the Fig. 4. As a result of comparison, the thermal distribution on the plate was found to be 2,024 ºC at heat speed of 3 mm/sec. But the maximum heat distribution was found as 2,011 ºC by using the thermal camera as represented in Fig. 5. From the result, very close difference is obtained as 13 ºC. It is due to some of the reason such as the content of the air, availability of the shielding gas required for the welding and the distance between thermal camera and plates. The minimum temperature of plate was found as 337 ºC and by thermal imaging camera it was obtained as 91 ºC. This difference is obtained due the atmospheric temperature. From the thermal distribution analysis, it can be clearly seen that temperature decreases with increase in the welding speed.

Thermal Analysis During Welding

Thermal analysis study is significant in observing the temperature distribution during welding. Hence, the Infra-red thermography is carried out to perform the thermal analysis during the welding process. It is a renowned methodology and beneficial in capturing the

temperature in the range of twenty to two hundred degree Celsius. An infra-red photo imager is fixed with the data collector to analyze the temperature distribution over the welding field. Snapshots are created using the above setup to observe the distribution of temperature. Fig. 6 represent the temperature distribution of the welding element

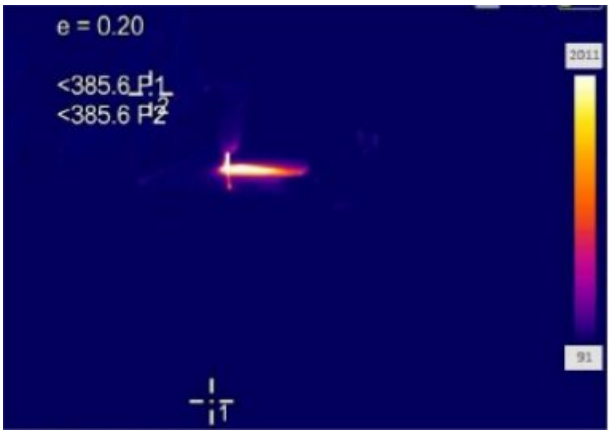

Fig. 5. Temperature measurement of AISI304 and SA213T22 TIG Welding by using thermal camera.

Table 12. Temperature distribution across the welding

Method Welding routes		Temperature (°C)		
		14 s	28 s	56 s
TIG	Rooting	1459	1495	1642
	Filling	1545	1590	1695
	Capping	1730	1755	1816

Conclusion

In this present research work TOPSIS technique was used to optimize the process parameters of CO_2 laser beam welding on cupronickel alloys. Four input variables namely laser power, welding current, welding angle and welding speed with two different levels were considered. These four important process parameters are optimized based on the output parameters viz hardness, tensile, yield and energy. Further these experiment results are processed through TOPSIS. By using this technique, welding specimen "**W5**" (Welding current 900 A, Welding angle 90°, Welding speed 1.4 mm/min and Laser power 30 w), was found to possess the best mechanical properties. It gained maximum overall weight of 0.715834995. The effects of input process parameters on output responses were investigated. The weld has been determined to be of good weld quality based on the mechanical properties of the welded specimen. TOPSIS approach is proven to be a valuable tool for optimizing the welding process parameters.

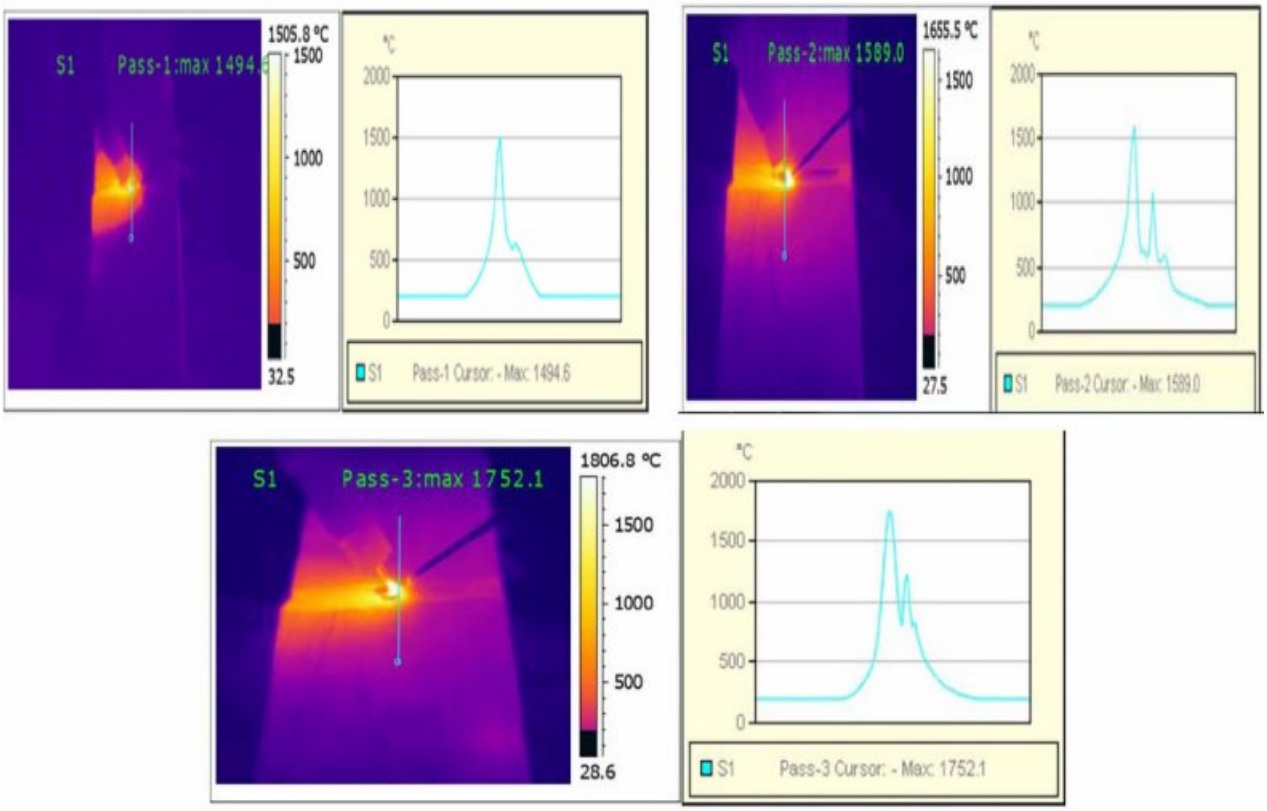

Fig. 6. Analysis of Temperature Distribution.

References

1. N. Saravanan, P. Ganeshan, B. Prabu, V. Yamunadevi, B. NagarajaGanesh, and K. Raja, J. Nat. Fibers (2021) 1-13.
2. M. Wahba, M. Mizutani, and S. Katayama, J. Mater. Eng. Perform. 25 (2016) 2889-2894.
3. V. Jeyabalaji, G.R. Kannan, P. Ganeshan, K. Raja, B. NagarajaGanesh, and P. Raju, J. Nat. Fibers (2021) 1-13.
4. K. Raja, V.S.C. Sekar, V.V. Kumar, T. Ramkumar, and P. Ganeshan, Arab. J. Sci. Eng. 45 (2020) 9481-9495.
5. P. Muthurasu and M. Kathiresan, J. Ceram. Process. Res. 22 (2021) 697-704.
6. S.A. Pichuzhkin, S.P. Chernobaev, A.A. Vainerman, and M.M. Veretennikov, Metallurgist 59 (2016) 968-973.
7. M.P. Chakravarthy, N. Ramanaiah, and B.S.K. Sundara Siva Rao, Proc. Inst. Mech. Eng. Part B J. Eng. Manuf. 228 (2014) 1153-1161.
8. C. Tan, L. Li, Y. Chen, and W. Guo, Mater. Des. 49 (2013) 766-773.
9. J. Shen, L. Wen, Y. Li, and D. Min, Mater. Sci. Eng. A 578 (2013) 303-309.
10. Y.B. Chen, J.C. Feng, L.Q. Li, Y. Li, and S. Chang, Int. J. Adv. Manuf. Technol. 68 (2013) 1351-1359.
11. M. Behzadian, S.K. Otaghsara, M. Yazdani, and J. Ignatius, Expert Syst. Appl. 39 (2012) 13051-13069.
12. M. Rajeshwaran, P. Ganeshan, and K. Raja, J. Appl. Fluid Mech. 11 (2018) 257-270.
13. V. Vignesh Kumar, K. Raja, T. Ramkumar, M. Selvakumar, and T.S. Senthil Kumar, Proc. Inst. Mech. Eng. Part E J. Process Mech. Eng. 235 (2021) 2180-2188.
14. P.G. Krishnan, B.S. Babu, and K. Siva, J. Ceram. Process. Res. 21 (2020) 157-163.
15. R. Pandiyarajan and M.P. Prabakaranb, J. Ceram. Process. Res. 21 (2020) 690-698.
16. B.R. Kumar, N. Chauhan, and P.M. Raole, *Adv. Mat. Res.* 585 (2012) 430-434.
17. A. Belhadj, J.-E. Masse, L. Barrallier, M. Bouhafs, and J. Bessrour, J. Laser Appl. 22 (2010) 56-61.
18. P. Ferro, F. Bonollo, and A. Tiziani, Sci. Technol. Weld. Join. 10 (2005) 299-310.
19. V. Yamunadevi, K. Palaniradja, A. Thiagarajan, P. Ganeshan, and K. Raja, Mater. Res. Express 6 (2019) 95057.
20. G. Radhaboy, M. Pugazhvadivu, P. Ganeshan, and K. Raja, Energy Sources, Part A Recover. Util. Environ. Eff. (2019).
21. V.V. Kumar, K. Raja, V.S.C. Sekar, and T. Ramkumar, J. Brazilian Soc. Mech. Sci. Eng. 41 (2019) 1-14.
22. B. Suresh Babu, C. Gb, C. Boopathi, T. Pridhar, and R. Srinivasan, J. Ceram. Process. Res. 19 (2018) 69-74.
23. C. Chanakyan and S. Sivasankar, J. Ceram. Process. Res. 21[6] (2020) 647-655.
24. L. Shi, J. Chen, C.S. Wu, and L. Fu, Sci. Technol. Weld. Join. 26 (2021) 363-370.
25. M. Gao, X.Y. Zeng, and Q.W. Hu, Sci. Technol. Weld. Join. 11 (2006) 517-522.
26. N. Selvakumar, B. Gnanasundarajayaraja, and P. Rajeshkumar, Exp. Tech. 40 (2016) 129-135.
27. P. Ferro, F. Bonollo, and A. Tiziani, Sci. Technol. Weld. Join. 10 (2005) 299-310.
28. K.A.S. Lewise and J.E.R. Dhas, Mater. Manuf. Process. 37 (2022) 34-42.